Effective Thermal Conductivity of Sintered Heat Pipe Wicks

G. P. Peterson* and L. S. Fletcher†
Mechanical Engineering Department, Texas A & M University, College Station, Texas

The effective thermal conductivity of sintered metal materials similar to those used in heat pipe wicks has been investigated. Experimental tests were conducted using both sintered Nickel 200 and sintered copper powders over a temperature range of 25°C to 100°C. Data were obtained for samples with several porosities in both dry and water-saturated conditions. The effective thermal conductivity of the sintered materials was found to be a function of the thermal conductivity of the solid material from which the sintered metal was made, the porosity, the mean sample temperature, and whether the material was dry or saturated. The results of the experimental investigation are presented and compared with the experimental results and analytical solutions of other investigators.

Nomenclature

b = dummy variable
c = dummy variable
k_e = effective thermal conductivity
k_ℓ = thermal conductivity of the liquid
k_s = thermal conductivity of the solid
r = radius of the contact point
R = radius of the powdered particles
x = dummy variable
α = experimental parameter
β = $(1-\nu)/(1+\nu)$
ε = porosity
ν = k_ℓ/k_s
ρ_b = bulk density of the sintered material
ρ_g = density of the solid material

Introduction

In a heat pipe, the effective capillary pore radius of the wick structure determines the capillary pumping capability and hence, the overall heat transport capacity. Reductions in the capillary radius may increase the capillary pumping pressure, but at the same time may also increase the axial pressure gradient due to a reduction in the wick permeability.

A number of different types of wicking structures have been developed and tested over the past twenty years. Wick structures made of layers of wire screen or metal felt, axial and/or circumferential grooves, and sintered wicks are all commonly used in various types of heat pipes.[1] Sintered heat pipe wicks, which are normally made from some type of sintered metal fiber or powder, have an effective capillary pore radius significantly smaller than either wrapped screen or axially grooved heat pipes, and as a result have seen limited use due to the increased axial pressure gradient.[2] The recent development of several innovative heat pipe designs, which allow axial and radial liquid flow to occur independently, have made the use of sintered wicks increasingly attractive. Sintered wicks, when combined with one of these new designs, offer a means by which the capillary pumping capability can be increased without increasing the axial pressure gradient.[3]

Of equal importance in heat pipe wicks is the temperature drop occurring between the outside surface of the heat pipe casing and the liquid meniscus formed at the liquid-vapor interface.[4] In this area, sintered materials offer two significant advantages over the other wick structures mentioned previously. First, the effective thermal conductivity of the sintered material, which is normally defined as the ratio of the total heat flux to the average temperature gradient, is much higher than that occurring in other types of wicks. Second, since the material comprising the wick is sintered directly to the interior of the heat pipe casing, the thermal contact resistance is greatly reduced. This decreased contact resistance, along with the relatively high thermal conductivity of the sintered materials, results in a decrease in the temperature drop occurring between the outside of the heat pipe case and the liquid-vapor interface. Consequently, higher evaporator heat fluxes can be attained, prior to the onset of nucleate boiling in the wick.[5]

Because of the increased utilization of sintered materials for heat pipe wicks and the significance of the effective thermal conductivity on heat pipe operation, a review of both the experimental and analytical work involving the effective thermal conductivity of sintered materials was conducted. Based upon this review, it was apparent that additional experimental data are necessary, particularly in the area of sintered metal powders. Hence, an experimental investigation was undertaken to obtain test data for use in evaluating the existing models.

Literature Review

Sintered metal materials may be divided into two major categories, sintered metal fibers and sintered metal powders. Within these two categories, different material densities are subdivided according to the porosity of the sintered material, ε, which is defined by the following relationship

$$\varepsilon = 1 - (\rho_b/\rho_g) \tag{1}$$

The simplest analytical configurations used to model the effective thermal conductivity of these materials take into account the material porosity, but do not differentiate between the sintered fiber and the sintered powder materials. In these models, the solid and liquid phases are assumed to be either in pure series or parallel in which cases the effective thermal conductivity may be written as

$$k_e = \frac{k_\ell k_s}{\varepsilon k_s + k_\ell(1-\varepsilon)} \tag{2}$$

Received June 6, 1986; revision received Oct. 5, 1986. Sponsored in part by the Mechanical Engineering Division of the Texas Engineering Experiment Station.

*Assistant Professor of Mechanical Engineering. Member AIAA.
†Associate Dean of Engineering and Professor of Mechanical Engineering. Fellow, AIAA.

or

$$k_e = \varepsilon k_\ell + (1-\varepsilon)k_s \tag{3}$$

respectively.

These two equations provide an upper limit in the case of the parallel approximation, and a lower limit in the case of the series approximation.[6] However, neither solution appears to provide an accurate method for predicting the effective thermal conductivity of saturated sintered materials. An excellent summary of other general analytical methods for determining the thermal conductivity of sintered materials is presented by Alexander.[7]

Sintered Metal Fiber Wicks

The effective thermal conductivity of sintered metal fiber materials has been investigated by a number of individuals, with a majority of the work having been concerned with the conductivity along rather than across the fibers. The previous analytical work, once assimilated and compared, can be condensed into a set of six separate solutions, three of which are exact analytical solutions and three of which are empirical in nature.

At the turn of the century, Rayleigh[8] developed a series solution for computing the effective thermal conductivity of a square array of uniformly sized cylinders using potential theory.

$$\frac{k_e}{k_s} = 1 - \frac{2\varepsilon}{\beta + \varepsilon - \dfrac{0.036\varepsilon^4}{\beta} - \dfrac{0.0134\varepsilon^8}{\beta} - \ldots} \tag{4}$$

where $\beta = (1-v)/(1+v)$ and $v = k_\ell/k_s$.

Maxwell[9] has presented an expression for a random distribution of cylinders far enough apart, that no interference occurs between the cylinders. This expression,

$$\frac{k_e}{k_s} = \frac{\beta - \varepsilon}{\beta + \varepsilon} \tag{5}$$

is identical to Eq. (4) except that the ε^4 and higher terms, which compensate for the interrelational effects of the cylinders, have been omitted. In addition to these two expressions, Deissler developed an expression for the heterogeneous conductivity of square and triangular arrays of cylinders in point contact using a relaxation technique.[10] More recently, experimental work performed by Soliman et al.,[11] Singh et al.,[12] and Alexander[7] have produced empirical expressions for predicting the effective thermal conductivity of water-saturated sintered metal fiber materials in the direction of the fibers.

These expressions are respectively,

$$\frac{k_e}{k_s} = 0.455(1-v)(1-\varepsilon)^{1.36} + v\left\{1 + \frac{(1-v)[(1-\varepsilon) - 0.455(1-\varepsilon)^{1.36}]}{[1-(1-v)(1-\varepsilon)^{0.015}]}\right\} \tag{6}$$

where $v = k_\ell/k_s$

$$\frac{k_e}{k_s} = \left[1 - \varepsilon + \frac{k_\ell}{k_s}\varepsilon \exp[(1-\sqrt{k_\ell/k_s})^b]\right] \exp[-\varepsilon(1-\sqrt{k_\ell/k_s})^b] \tag{7}$$

where $b = 20\sqrt{k_\ell/k_s}$

and

$$k_e = k_\ell \left(\frac{k_s}{k_\ell}\right)^{(1-\varepsilon)^\alpha} \tag{8}$$

where the exponent α is 0.34 for fiber or felt metal wicks. All three of these expressions are based upon limited amounts of experimental data, with at most four data points available for each one.

Figures 1 and 2 illustrate the relationships that exist between the parallel model and the empirical prediction correlations developed by Soliman et al.,[11] Singh et al.,[12] and Alexander.[7] Also shown are the experimental values obtained by each of these investigators.

As mentioned previously, the parallel approximation provides an upper bound for the effective thermal conductivity, and greatly overestimates the experimental values obtained for a given porosity. Maxwell's method, Eq. (5), falls below the values obtained using the parallel model, but still overestimates the results of the existing experimental work.

As shown in Fig. 1, there is considerable variation in the experimental values obtained for the thermal conductivity, by the different investigators, particularly at porosities slightly higher than 80%. This variation has, in the case of the Singh and Soliman data, been attributed to variations in the test apparatus and the experimental procedures used.[12] In comparing the experimental results of Soliman et al.[11] with the empirical expression developed by Singh et al.[12] for the Nickel 200 case, it can be seen that the data falls within 10%. No data is presented by Soliman et al.[11] for the case of sintered copper fiber materials along the fibers. The correlation developed by Alexander[7] is slightly higher than the experimental data for Nickel 200, and low for the available copper data, but overall it yields values within 20% of those measured.

In reviewing all of the experimental and empirical relationships developed thus far for sintered metal fiber materials, it is apparent that the correlation developed by Alexander[7] consistently yields the most accurate values.

Sintered Metal Powder Wicks

The analytical techniques used to develop expressions for the effective thermal conductivity of sintered metal powders are similar to those used for sintered metal fiber materials. Reimann[13] derived an exact solution for a cubic array of truncated spheres as

$$\frac{k_e}{k_s} = \left(\frac{R}{r} + \frac{1}{\pi}\ell n\frac{2R}{r}\right)^{-1} \tag{9}$$

where R is the radius of the spherical powdered particles and r is the contact radius. This expression assumes that the radius of the points of contact are small and known. In situations where the size of these contact points is not known, they can be estimated from a material balance as

$$\varepsilon = \left\{\frac{\pi}{6[1-(r/R)^2]^{2/3}}\right\}\left\{1 - \left(\frac{r}{R}\right)^2\left(2 - \sqrt{1-\left(\frac{r}{R}\right)^2}\right)\right\} \tag{10}$$

The combination of Eqs. (9) and (10) have been shown previously to average approximately 20% higher than experimental values for bronze, sandstone, and limestone.[8] As was the case with sintered metal fiber materials, Maxwell[9] has developed an expression for a regular array of uniformly sized

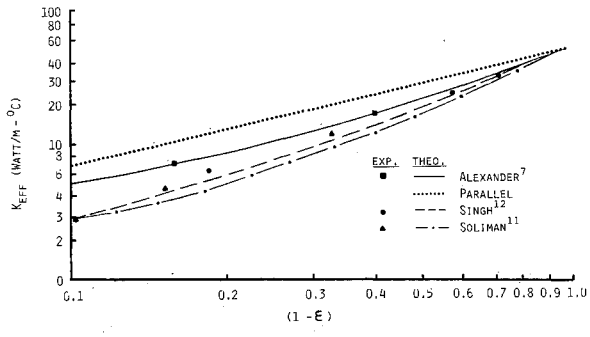

Fig. 1 Comparison of experimental and analytical results for water-saturated, sintered Nickel 200 fiber wicks.

spheres as,

$$\frac{k_e}{k_s} = \frac{2 + v - 2\varepsilon(1 - v)}{2 + v + \varepsilon(1 - v)} \tag{11}$$

More recently, Dul'nev[14] developed an analytical solution to determine the thermal conductivity of disperse systems having interconnected pores and pure unidirectional conduction.

$$\frac{k_e}{k_s} = \frac{c^2 + v(1 - c)^2 + 2vc(1 - c)}{1 - c(1 - v)} \tag{12}$$

where

$$c = \frac{x/(0.5 - x)}{1 + (x/(0.5 - x))} \tag{13}$$

and x is found from

$$4x^3 - 3x^2 + \frac{1 - \varepsilon}{4} = 0 \tag{14}$$

which yields two positive real values, the larger of which should be used. Although this solution was developed for disperse systems, it has been used by both Soliman et al.[11] and Singh et al.[12] to predict the effective thermal conductivity of sintered metal fiber materials and in some cases was reasonably accurate. Finally, Alexander[7] used the same expression developed for sintered fibrous materials, Eq. (8), for sintered powders, but substituted a value of 0.53 for the exponent α.

Experimental Investigation

Experimental Test Facility

The experimental facilities used in this investigation, along with the details of the facility construction, operation, and accuracy, have been reported previously by Miller and Fletcher.[15] The apparatus which is shown in Fig. 3, consisted of a horizontal column composed of a heat source, the two metal test fixtures, the sintered wick specimen, and a heat sink. The test fixtures and wick specimen were arranged so that a cylinder of the sintered material was "sandwiched" between the two metal test fixtures and encased in a Teflon tube. The heat source was a 300-W band heater attached to one of the test fixtures. To eliminate axial heat losses in the test fixture, radiation shield heaters were attached to both ends of the test column. Radial heat losses were monitored by a thermocouple on the surface of each of the test fixtures and losses from the test fixtures and test specimen were minimized by placing radiation shields, made of high emissivity, low absorptivity material and asbestos, around the test column. In addition, a 200-W radiation shield heater was placed around the high temperature end of the test fixture, outside of the radiation shield.

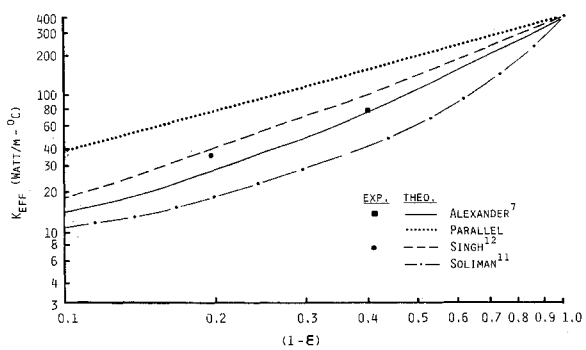

Fig. 2 Comparison of experimental and analytical results for water-saturated, sintered copper fiber wicks.

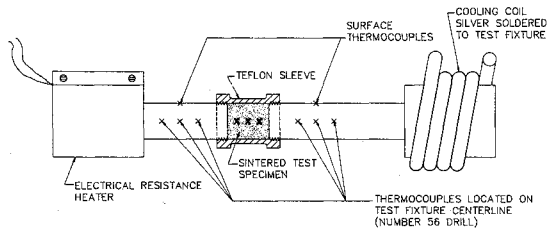

Fig. 3 Experimental test apparatus.

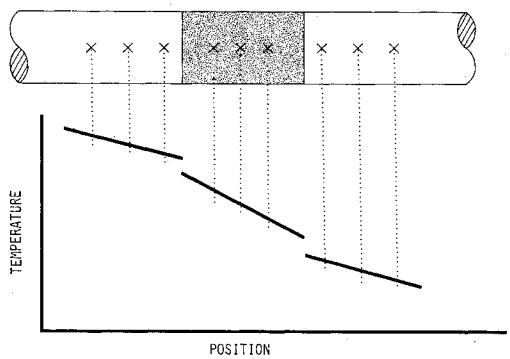

Fig. 4 Temperature distribution.

To determine the thermal conductivity of the test specimen, three chromel-alumel (AWG-30) thermocouples were located along the centerline of each of the two test fixtures, 1.27 cm apart. Three additional thermocouples were located along the centerline of each of the test specimens, 0.635 cm apart. The thermocouples were secured in the holes (No. 56 drill) with a metal filled epoxy. Using the temperatures obtained from these thermocouples and the known thermal conductivity of the test fixtures, the heat flux through the test column could be determined as shown in Fig. 4. With the heat flux and the temperature distribution known, the effective thermal conductivity of the test specimen could be determined. Because of the low thermal conductivity and the small cross-sectional area, the heat conducted through the Teflon sleeve was considered negligible.

The thermal conductivity tests were conducted in a vacuum environment to eliminate the conduction and convection losses to the surrounding air and also to eliminate the effects of any interstitial fluids on the thermal conductivity. A vacuum of 1.33×10^{-3} N/m^2 was maintained using a General Scientific model D500 roughing pump in series with an NRC VHJ-6 oil diffusion pump. A 46 × 76 cm Pyrex bell jar was used to encase the test facility. Four NRC model 531 thermocouple gauges, in conjunction with two Bayard-Alpert ionization gauge tubes and an ion gauge controller, were used to monitor the vacuum quality.

Experimental Procedure

Six test specimens, three each of Nickel 200 and Copper C102 sintered powders were machined to the correct dimensions on a lathe without the use of coolants or lubricants. Because most conventional cutting operations result in some degradation of the cut surface, usually in the form of a burnished or densified region along the edge, each of the machined surfaces were examined and photographed under a microscope as shown in Fig. 5. After examining these photomicrographs, it was apparent that the densified region was confined to a very small area near the cut edge and therefore, the effects of the machining process on the porosity measurements could be considered negligible.[16]

After the samples had been prepared, the porosity was measured using the density method.[17] Using the known density of

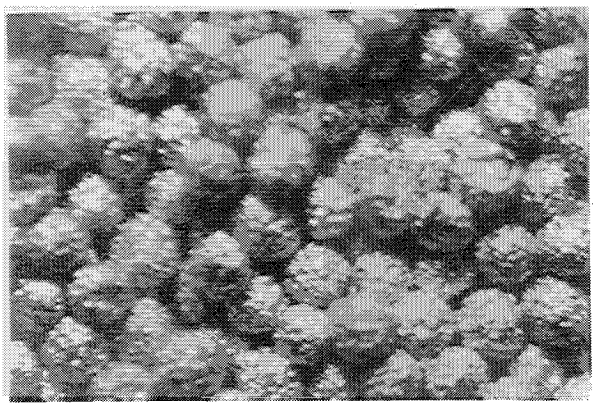

Fig. 5 Photomicrograph of a sintered powder specimen.

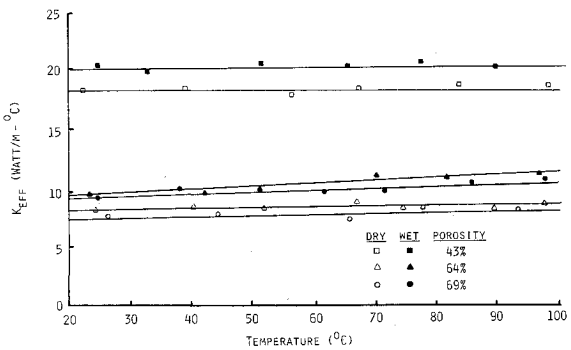

Fig. 6 Effect of temperature on the effective thermal conductivity of sintered Nickel 200 powder wicks.

the sintered powder, and the measured bulk density, the porosity could be determined from Eq. (1). Table 1 lists the results of these porosity measurements along with the other important parameters for each of the test specimens. With the exception of the porosity, all of the data listed in Table 1 were provided by the sintered material manufacturer.

Tests to determine the effective thermal conductivity of the test specimens with no interstitial gases present were conducted first, in order to eliminate the effects of any deposits which might be left from the saturated tests. For these dry tests, the fixtures were cleaned with acetone and assembled. The air present in the pores of the sintered material was allowed to escape through a vent hole in the Teflon sleeve, once the sample had been installed in the vacuum facility. In the saturated tests, the wick was soaked in distilled water to ensure that it was fully wetted and then the test fixtures were assembled with the excess water flowing out of the sintered material through the vent hole in the Teflon sleeve. After the test column was fully assembled, the vent hole was sealed using an epoxy cement.

Once the test specimen and test fixtures had been instrumented and installed in the test facility, the radiation shields were put in place and the system was pumped down to a vacuum of 1.33×10^{-3} N/m^2. After outgassing, the test specimens were raised to the desired temperature by adjusting the heater controls. Data were taken over a temperature range of 25°C to 100°C, which is within the normal operating range for heat pipes using water as the working fluid. To ensure that a steady-state condition had been achieved, data were taken when the temperature did not vary more than 0.5°C over a 45-min interval. This steady-state procedure took approximately 12 h.

Results and Discussion

Tests were conducted with each of the test specimens to determine what effect variations in the mean specimen temperature would have on the effective thermal conductivity. Figures 6 and 7 illustrate the results of these tests for the sintered Nickel 200 and the sintered Copper C102 samples, respectively. The solid symbols represent the saturated data and the open symbols represent the dry or vacuum data. As shown, the effective thermal conductivity for the sintered copper is significantly higher than for the sintered Nickel 200 materials. This result is not surprising since the bulk thermal conductivity of the Copper C102 is almost six times higher than for Nickel 200. It can also be seen that the effective thermal conductivity for both types of material, increases slightly with a corresponding increase in the average specimen temperature.

When tested in a water-saturated condition, both the Nickel 200 and the Copper C102 test specimens demonstrated a similarly increasing trend with respect to temperature. In addition, the effective thermal conductivity increased significantly due to the presence of the water in the pores of the sintered material. These two tendencies, a slight increase in the effective thermal conductivity with respect to temperature, and a significant increase in the effective thermal conductivity of the saturated materials, were evident in all of the specimens tested.

Figures 8 and 9 compare the results of the experimental investigation with several of the modeling techniques described previously. As can be seen, the parallel model once again significantly overestimates the measured values and is of little use except in defining the upper limit. The expression developed by Maxwell, Eq. (11), although somewhat better than the parallel model, still overestimates the experimental results by as much as 40%. In comparing the experimental results with the values obtained using the prediction techniques developed by Dul'nev[14] and Alexander,[7] it can be seen that the expression developed by Dul'nev[14] is better than either the parallel approximation or the Maxwell correlation, but still overestimates the results obtained in the experimental investigation. The expression developed by Alexander,[7] however, is extremely close to the experimental data obtained for the Nickel 200 specimens and slightly low for the Copper C102 specimens.

In comparing the results of this experimental investigation, Figs. 8 and 9, with the results of previous experimental investigations performed on sintered fiber materials, Figs. 1 and 2, it can be seen that the effective thermal conductivity of the sintered metal fiber materials, along the fibers, is slightly higher

Table 1 Wick samples and their properties

Wick	Mesh range[a]	Permeability[a]	Pore radius[a]	Porosity[b]
Ni 200	60/80	1.2×10^{-7} cm^2	0.0034 cm	69%
Ni 200	80/150	1.5×10^{-7} cm^2	0.0034 cm	43%
Ni 200	250/325	2.0×10^{-7} cm^2	0.0035 cm	64%
Cu C102	100/170	9.3×10^{-8} cm^2	0.0036 cm	59%
Cu C102	170/200	5.5×10^{-8} cm^2	0.0037 cm	52%
Cu C102	325/–	1.2×10^{-9} cm^2	0.0033 cm	32%

[a]Data provided by Thermacore Inc. [b]Measured values from this investigation.

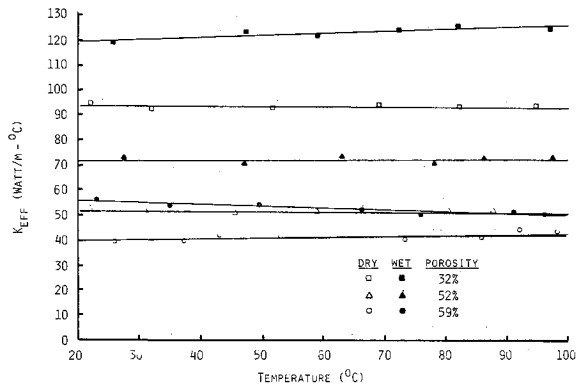

Fig. 7 Effect of temperature on the effective thermal conductivity of sintered Copper C102 powder wicks.

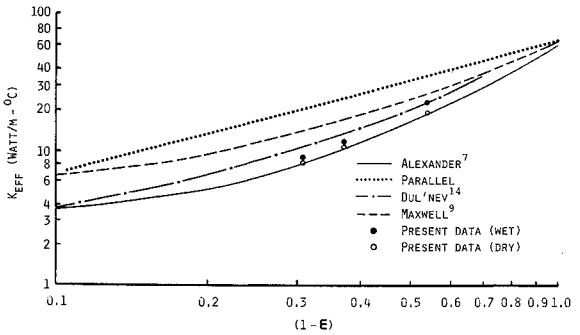

Fig. 8 Comparison of experimental results and analytical predictions for sintered Nickel 200 powder wicks.

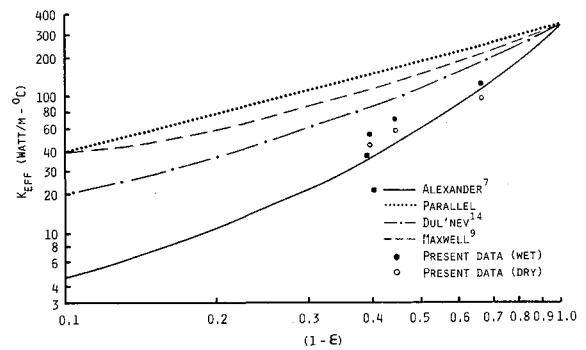

Fig. 9 Comparison of experimental results and analytical predictions for Copper C102 powder wicks.

Conclusions and Recommendations

The experimental program described here has used the steady-state method to determine the effective thermal conductivity of both dry and water-saturated sintered powdered heat pipe wick materials. It has been demonstrated that the effective thermal conductivity is a function of the thermal conductivity of the metal from which the sintered powder is made, the thermal conductivity of the fluid filling the pores, if any is present, the porosity, and the mean specimen temperature.

The results of the experimental program when compared with the existing analytical solutions of other investigators, indicates that although none of the methods give uniform agreement, the method developed by Alexander[7] very closely approximates the experimental results obtained for sintered Nickel 200 powders, but is somewhat low for the Copper C102 data. The relationship developed by Dul'nev[14] for sintered powders, while as accurate as the Alexander correlation for Copper C102, somewhat overestimates the values for Nickel 200.

Based upon the results of this work, it is apparent that additional investigations are required to improve the existing expressions for anisotropic materials, such as felt metals or multilayer screens. It is also recommended that additional experimental tests be conducted on both sintered metal fiber and sintered metal powder samples over a wider range of porosities and that other types of heat pipe wick materials be evaluated. Once additional experimental data are available, comparisons should be made with the existing correlations.

Notes

The authors would like to thank Thermacore Inc. for their assistance in supplying the test materials. Work sponsored in part by the Mechanical Engineering Division of the Texas Engineering Experiment Station.

References

[1]Dunn, P. D. and Reay, D. A., *Heat Pipes*, 2nd edition, Pergamon, New York, 1978, pp. 68–70.

[2]Ivanovskii, M. N., Sorokin, V. P., and Yogodkin, I. V., "Processes in Heat Pipes," *Transactions of the Physico-Energetics Institute*, Atomizdat, Moscow, 1974, pp. 271–286.

[3]Shaubach, R. M., "High Performance Ambient Temperature Heat Pipes," Project Summary, NASA Contract # SBIR 09-08-6551, 1985.

[4]Cotter, T. P., "Theory of Heat Pipes," Los Alamos Scientific Laboratory Technical Report # LA-3246-MS, Feb. 23, 1965.

[5]Chi, S. W., *Heat Pipe Theory and Practice*, McGraw-Hill, New York, 1976, pp. 160–162.

[6]Ferrell, J. K., Alexander, E. G., and Piver, W. T., "Vaporization Heat Transfer in Heat Pipe Wick Materials," AIAA Paper 72-256, April 1972.

[7]Alexander, E. G. Jr., "Structure-Property Relationships in Heat Pipe Wicking Materials," Ph.D. Thesis, North Carolina State University, Dept. of Chemical Engineering, 1972.

[8]Rayleigh, L., "On the Influence of Obstacles Arranged in Rectangular Order Upon the Properties of a Medium," *Phil. Mag.*, Vol. 34, 1892, p. 481.

[9]Maxwell, J. C., *A Treatise on Electricity and Magnetism*, Vol. 1, 3rd Ed., Oxford Univ. Press, reprinted by Dover, New York, 1954.

[10]Gorring, R. L. and Churchill, S. W., "Thermal Conductivity of Heterogeneous Materials," *Chemical Engineering Progress*, Vol. 57, No. 7, July 1961, pp. 53–59.

[11]Soliman, M. M., Graumann, D. W., and Berenson, P. J., "Effective Thermal Conductivity of Dry and Liquid-Saturated Sintered Fiber Metal Wicks," ASME Paper 70-HT/SpT-40, 1970.

[12]Singh, B. H., Dybbs, A., and Lyman, F. A., "Experimental Study of the Effective Thermal Conductivity of Liquid Saturated Sintered Fiber Metal Wicks," *International Journal of Heat and Mass Transfer*, Vol. 16, 1973, pp. 145–155.

[13]Reimann, G. H. M., "Die Partiellen Differential-Glechunger der Mathematischen Physik," Band 1, F. Vieweg and Sohn, Braunschweig, 1919, p. 474.

[14]Dul'nev, G. N., "Heat Transfer Through Solid Disperse Systems," *Inzhenero-Fizichweskii Zhurnal*, Vol. 9, No. 3, 1965, pp. 399–404.

[15]Miller, R. G. and Fletcher, L. S., "A Facility for the Measurement of Thermal Contact Conductance," *Proceedings of the Tenth Southeastern Seminar on Thermal Sciences*, New Orleans, Louisiana, April 1974, pp. 263–285.

[16]Miller, R. G. and Fletcher, L. S., "Thermal Contact Conductance of Porous Metallic Materials in a Vacuum Environment," *Progress in Astronautics and Aeronautics Thermophysics and Spacecraft Thermal Control*, Vol. 35, M.I.T. Press, Cambridge, June 1974, pp. 321–324.

[17]Scheidegger, A. E., *The Physics of Flow Through Porous Media*, University of Toronto Press, Toronto, Ontario, 1963, pp. 10–12.